Appearance Potentials of Field Ions

H. J. Heinen, F. W. Röllgen, and H. D. Beckey

Institut für physikalische Chemie der Universität Bonn

(Z. Naturforsch. **29 a**, 773–781 [1974]; received March 9, 1974)

The appearance potentials (AP) of various ions, which are produced by field ionization at platinum tip emitters have been measured by a retarding potential energy analyzer coupled to the output of a single-focusing magnetic mass spectrometer. Adsorption layers of water and organic molecules on the emitter surface were found to have no significant influence on the AP measurements.

The APs of the H_3O^+ and $(H_2O)_2H^+$ ions in the water spectrum and the $CH_3OH_2^+$ and $(CH_3OH)_2H^+$ ions in the methanol spectrum suggest that the emitter surface is involved in the protonation reactions. The APs of the other ions in the water and methanol spectra have also been studied.

The APs of the molecular ions of the paraffins allow conclusions to be drawn about the energy deposition function for field ionization. The fragment ions of n-heptane were found to have surprisingly low APs, up to 2.4-eV less than the molecular ion. The AP of the CH_3^+ ion in the methane spectrum indicates that it arises from a surface reaction.

Introduction

Investigations of the energy distribution of field ions and in particular the observation of resonances in the energy distribution of field ionized noble gas atoms and hydrogen molecules [1, 2] have revitalized the interest in the theory of field ionization (FI). In the energy analysis of ions other than those from the molecular peak the interest is focused on the appearance potential (AP). In analogy to other ionization methods, the AP for FI is defined as the minimum energy which must be supplied by the electric field in order to generate the ion concerned. This quantity determines the ionic energy deficit after FI corresponding to the potential at the points of generation of the ions. The AP allows conclusions to be drawn about the mechanism of the ion generation and about the desorption kinetics. The measurement of the APs of field ions also offers a possibility for determining the ionization potentials (IP) of molecules. Surface reaction products may have several APs if the ions are produced by several reaction mechanisms.

Previously, only a few APs of field ions have been measured, those of H_3O^+ (8.8 eV) and several water polymers [3], and that of H_3^+ (12.7 eV) [4], all formed by FI at tungsten surfaces. These low AP values indicate an involvement of the emitter surface in the protonation reaction. For example, in the case of the H_3^+ ion the reaction [5]:

$$2\,H_2 \xrightarrow{-e} {*}H + H_3^+ \qquad (1)$$

involves the simultaneous transfer of the proton and the bonding of a hydrogen atom to a radicalic center (*) of the emitter surface.

The present paper reports AP measurements of ions produced by the FI of substances which differ in their adsorption behaviour, i. e. noble gases, paraffins, water and methanol, at Pt-emitters. A further investigation concerns the extent to which the adsorbate coverage on the emitter surface influences the AP measurements of these molecules.

A single experimental arrangement for the simultaneous determination of the energy distribution and of the AP of field ions leads to unsatisfactory accuracy in the measurements. However, since in this work the AP was of predominant interest, the use of an energy analyzer working on the retarding potential principle was considered suitable [6]. Here the intensity of a field ion beam which has passed through a wire mesh retarding electrode is measured as a function of the difference of the potentials at the emitter (U_E) and the retarding electrode (U_R). The absolute value of the AP can be obtained simply from the cut-off point of the intensity function as [1]:

$$\mathrm{AP} = U_E - U_R + \Phi_R \qquad (2)$$

where Φ_R is the work function of the retarding electrode. In the case of the molecular ion $\mathrm{AP} = \mathrm{IP} + E_P$, where E_P is the polarization energy of the neutral molecule in the field. The polarization energy of the ion in the field has no effect on the measured AP,

Reprint requests to Prof. Dr. H. D. Beckey, Institut für Physikalische Chemie der Universität Bonn, *D-5300 Bonn*, Wegelerstrasse 12, Germany.

as it vanishes from the energy balance after removal of the ion from the high field.

The accuracy of the method is limited by the energy distribution of the electrons near the Fermi surface of the field anode, by the thermal energy of the ions, and by variations in the work function of the retarding electrode with adsorption layers. At room temperature the accuracy of the absolute AP measurements cannot be better than about ± 0.05 eV. For relative AP measurements a higher accuracy may be obtained when the energy distributions of the ions have the same shape.

No reliable measurements of the extent to which this condition is fulfilled have yet been made. However, it is reasonable to assume that the energy distribution of most ions at medium field strengths has a sharp maximum in the region of the highest energy as has been measured for H_2^+ [1] and He^+ [7]. The exact energy distribution depends on the type of the ion generation process involved and probably also on the coverage of the surface with adsorption layers. The "onset" method chosen for this study has the particular advantage that the dependence of the AP measurements on the energy distributions of the various ions is smaller than that of an AP determination from the intensity maximum in the energy distribution.

Although the measurements do not allow quantitative conclusions about the energy distributions of the ions to be made, nevertheless characteristic differences in these distributions for the various ions are clearly distinguishable.

Experimental

The experimental arrangement for measuring APs is shown schematically in Figure 1. The energy analysis is made after magnetic mass separation. Placing the energy analyzer in front of the magnet reduces the accuracy of measurement of the APs, since at the high retardations involved the focusing of the ion beam after the retardation electrode is unsatisfactory for magnetic mass separation. The retardation electrode consists of two gold meshes, each of 20 squares per linear millimeter and 70% transmission, placed 2 mm apart. The constancy of the work function is optimal for gold. Under the chosen experimental conditions (potential at the retarding electrode 2.5 kV) the penetration through the two meshes was estimated not to exceed 0.05 eV.

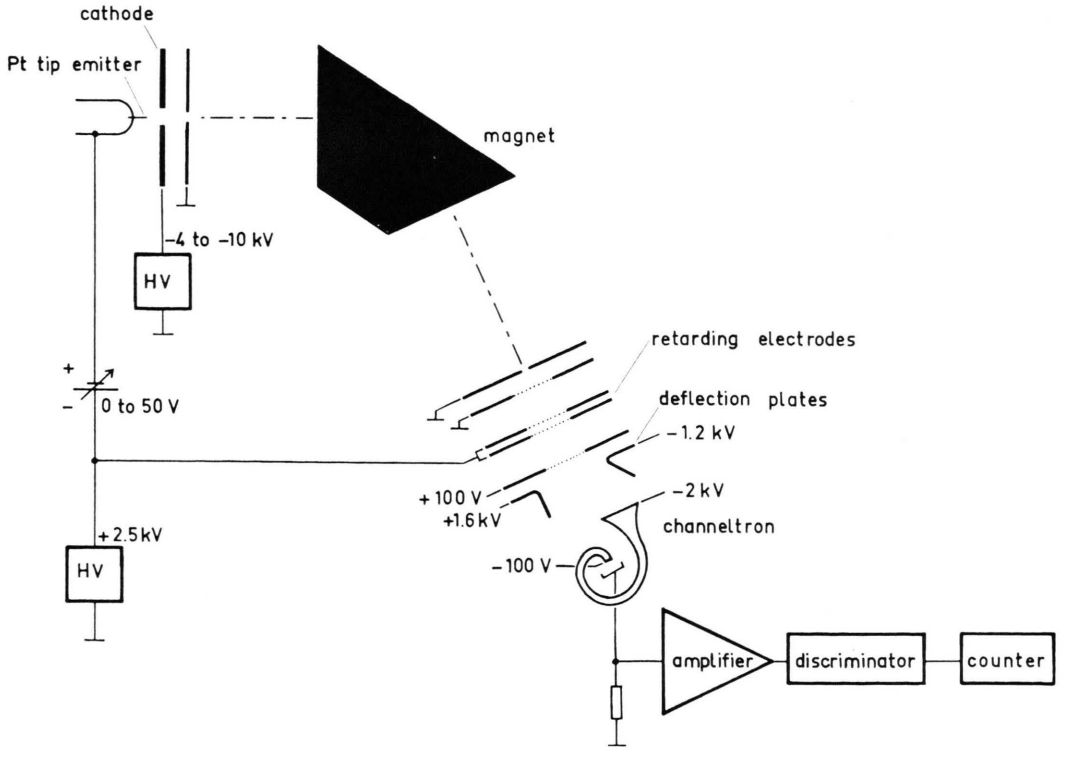

Fig. 1. Experimental assembly (schematic).

The ion detector, a channeltron, was offset from the optical axis to avoid the background signal arising during the retardation of the highly energetic ions. Ions reflected from the retardation electrode release secondary electrons, which are accelerated by the electrode meshes and in their turn generate bremsstrahlung or release secondary ions by impact-induced desorption. By offsetting the detector from the optical axis the radiative component of the background signal, which is of the same order of magnitude as the primary ion signal, could be largely eliminated. However, the secondary ions are accelerated together with the transmitted primary ions, deflected onto the detector, and thus still produce a background signal. It was observed that this signal depends on the type of primary ion and is generally proportional to the primary ion intensity. The ratio of the primary ion signal to the background signal lies between 10^4 and 10^3 at sufficiently large primary ion intensities, but is lower at small primary ion intensities because of the noise of the channeltron itself.

The "retardation curves" discussed below were obtained in the following manner. The magnetic field was first adjusted to the peak maximum and then the detector signal was measured as a function of the potential difference between the retardation electrode and the field anode. No difference was found between the curves obtained in this way and those obtained by integrating the intensity over the whole peak width. It was observed that the magnetic sector in front of the energy analyzer behaves as an energy filter with peak half-width ≈ 20 eV for ions of constant mass. In order to make use of the full dynamic range available, counting techniques were employed.

To determine the cut-off point in the retardation curves the intensity was plotted logarithmically. This reveals fine structures in the intensity distribution near the cut-off point more clearly and also produces a particularly steep curve at this point. Thus its determination is less dependent upon the energy distribution of the field ions and on the signal to noise ratio. Where several ion generation mechanisms with different APs for a single ion species exist, the curves obtained consist of several superimposed retardation curves. The cut-off points corresponding to the APs are shifted to higher values on the logarithmic diagram. However, the correct results may be obtained by deconvolution. Accuracy of measurement is lower in this case because of the smaller difference between the ion signal and the background.

Measurements with various Pt-emitters gave the same retardation curves and the same APs within the limits of accuracy of the experiments. The field strength was adjusted by means of the emitter-cathode potential difference so that a high ion emission was obtained, but no measurable preionization in front of the emitter took place. Under these conditions no dependence of the AP on the field strength was observable.

Results

Xenon, Krypton and Argon

Figure 2 shows the retardation curves of xenon (m/e 129) and krypton (m/e 84). The ratio of the primary ion current to the background current was larger for Kr than for Xe. The shapes of the curves are similar and no differences in the energy distributions could be detected.

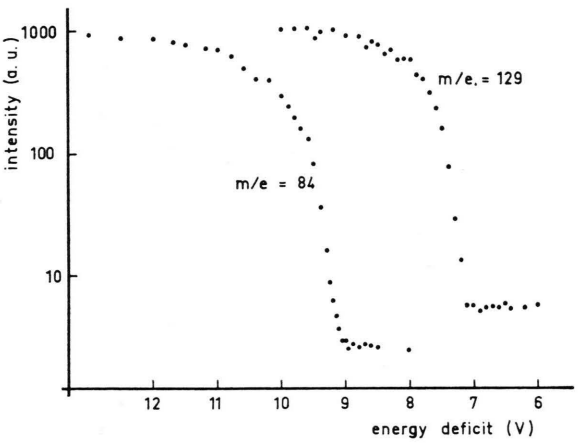

Fig. 2. Retardation curves of field ionized xenon and krypton.

The energy deficit $\Delta U = U_E - U_R$ is 7.2 ± 0.1 eV for xenon and 9.1 ± 0.1 eV for krypton. Within the accuracy of the measurements the difference of the ΔU values is equal to that of the ionization potentials of the two gases (12.1 eV and 14.0 eV). The work function of the retardation electrode is thus determined to be $\Phi_R = 4.9 \pm 0.1$ eV. For argon a value of $\Delta U = 10.9 \pm 0.1$ eV, corresponding to an IP of 15.8 eV, was obtained.

In order to investigate the influence of organic or water adsorption layers on the AP measurements mixtures of Xe with n-heptane, and Xe with water, both in the ratio 1:1, were admitted to the MS via the gas inlet system during separate experiments. It is known that water and even paraffins [8] produce adsorption layers on the emitter surface under the conditions of FI. The AP of Xe was found to be unaffected by the presence of n-heptane or water.

Paraffins

The retardation curves of the molecular ions (M^+) of the paraffins have the same shape as those of the noble gases (see Figure 3). However, a remarkable difference between the measured APs of M^+ paraffin ions and those of noble gas ions was observed. The APs of the M^+ paraffin ions are consistently some tenths of an eV too high when compared with literature values[9] of the IP of the same molecules (see Table I). Even these IPs, determined by photo ionization, exceed the adiabatic IPs[10]. As mentioned above, this effect cannot be ascribed to an alteration of the work function of the retarding electrode, nor to the influence of surface layer formation on the emitter. The high AP values were also found not to result principally from the polarization energy E_p of the molecules, since for benzene no AP higher than the IP can be detected, although benzene has about the same molecular polarizability as heptane. The higher APs must have their origin in the FI process itself.

The retardation curves of the fragment ions of n-heptane are shown in Figs. 3, 4 and 5. The shape of the curve for the $C_2H_5^+$ ion is different from the rest and is considerably flatter. The APs of the

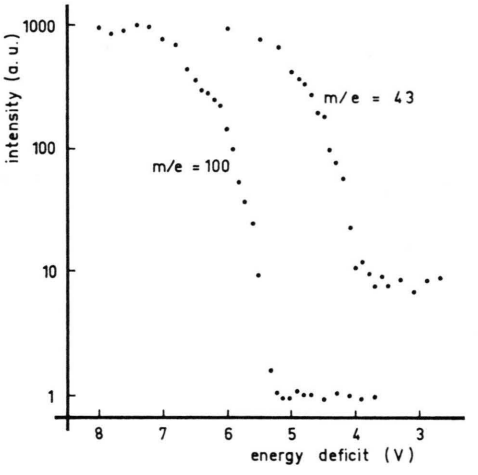

Fig. 3. Retardation curves of field ionized n-heptane: $C_7H_1^+$ and $C_3H_7^+$.

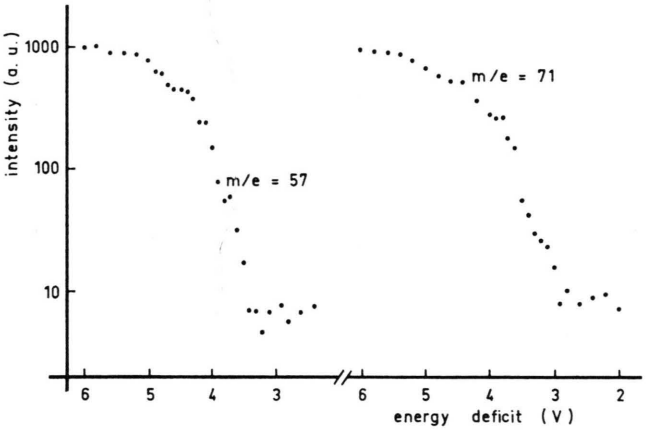

Fig. 4. Retardation curves of field ionized n-heptane: $C_4H_9^+$ and $C_5H_{11}^+$.

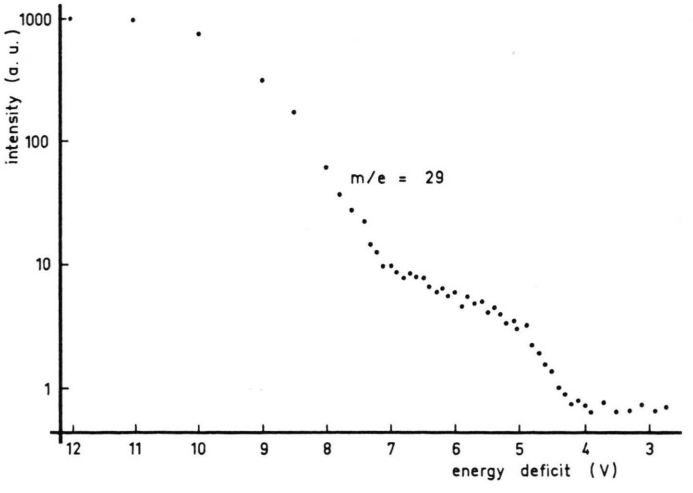

Fig. 5. Retardation curve of field ionized n-heptane: $C_2H_5^+$.

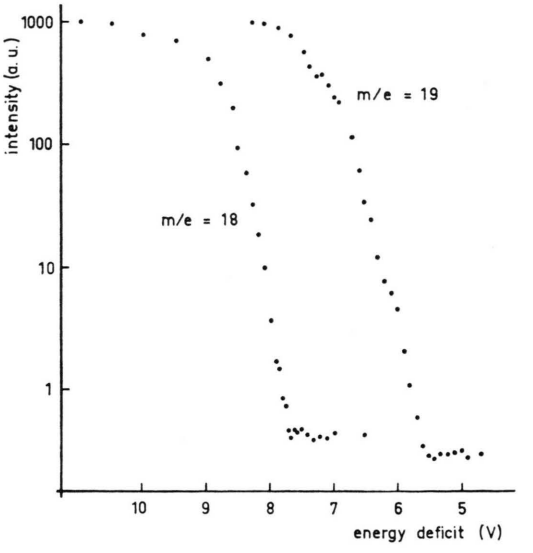

Fig. 6. Retardation curves of field ionized water: H_2O^+ and H_3O^+.

n-heptane fragment ions are all below the AP of the heptane molecular ion (Table I). Assuming that an AP may be assigned to the second step in the curve of m/e 29 (Fig. 5), a value about 2 eV above the AP of the molecular ion is obtained. In all the tables the relative intensities of the mass peaks are given in brackets.

Similarly the CH_3^+ ion in the methane spectrum is not a monomolecular decomposition product, since its AP is noticeably lower than the AP of the methane molecular ion.

Water

Water shows a tendency to the formation of multilayers and clusters on the emitter surface. Figures 6 and 7 show the retardation curves of masses 18 (H_2O^+), 19 (H_3O^+), 36 ($H_4O_2^{+\cdot}$) and 37 ($H_5O_2^+$) in the water spectrum.

The APs of the ions of the water spectrum, including that of m/e 32 ($O_2^{+\cdot}$) and m/e 50 (probable structure: $H_2O \cdot O_2^{+\cdot}$), which also appeared in the water MS during FI at Pt (see Ref. [11]), are shown in Table II. The AP of $O_2^{+\cdot}$ corresponds to the IP of O_2 within the accuracy of the experiment.

Methanol

Figures 8 to 11 show the retardation curves of the ions in the methanol spectrum. The corresponding APs are listed in Table III. As may be determined from the relative ion intensity of the mass peaks the ion currents at masses 31, 32, and 33

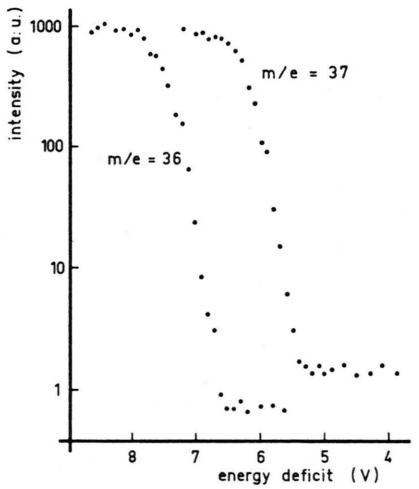

Fig. 7. Retardation curves of field ionized water: $(H_2O)_2^{+\cdot}$ and $(H_2O)_2H^+$.

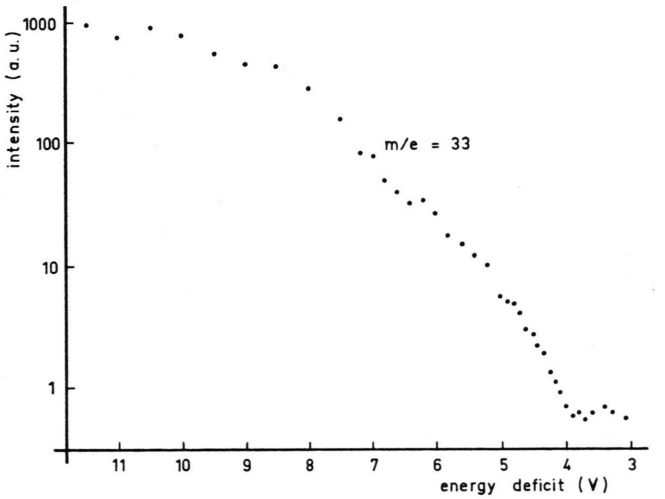

Fig. 9. Retardation curve of field ionized methanol: $CH_3OH_2^+$.

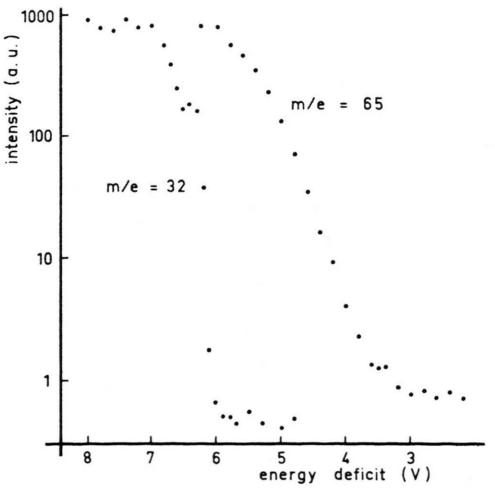

Fig. 8. Retardation curves of field ionized methanol: $CH_3OH^{+\cdot}$ and $(CH_3OH)_2H^+$.

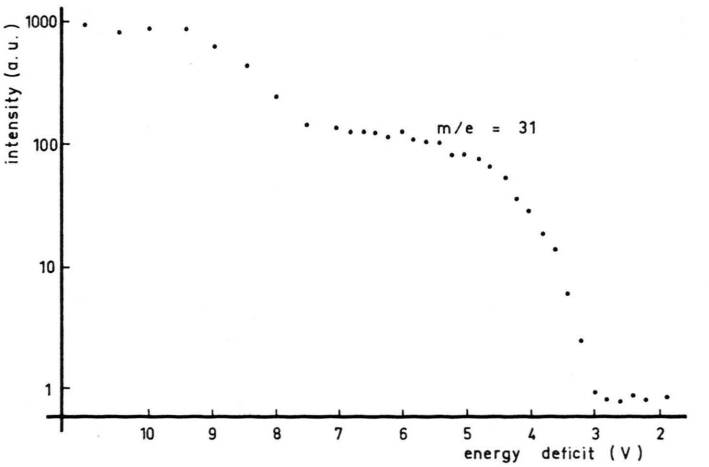

Fig. 10. Retardation curve of field ionized methanol: CH_2OH^+.

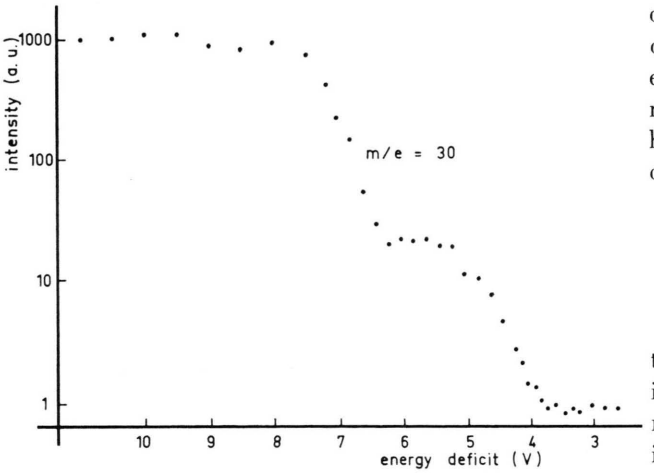

Fig. 11. Retardation curve of field ionized methanol: $CH_2O^{\cdot+}$.

Table I.

Substance	Ion (m/e)	ΔU (eV)	AP (eV)	IP (eV)
Methane	16 (≡100)	8.0 ± 0.1	12.9 ± 0.2	12.7 [9]
	15 (0.4)	5.9 ± 0.2	10.8 ± 0.3	
n-Hexane	86	5.4 ± 0.1	10.3 ± 0.2	10.18 [9]
n-Heptane	100 (≡100)	5.4 ± 0.1	10.3 ± 0.2	9.9 [9]
	71 (0.14)	3.0 ± 0.3	7.9 ± 0.4	
	57 (0.14)	3.5 ± 0.3	8.4 ± 0.4	
	43 (0.07)	3.9 ± 0.3	8.8 ± 0.4	
	29 (10)	4.2 ± 0.4	9.1 ± 0.5	
		7.2 ± 0.3	12.1 ± 0.3	
n-Octane	114	5.3 ± 0.1	10.2 ± 0.2	

Table II.

Substance	Ion (m/e)	ΔU (eV)	AP (eV)	IP (eV)
Water	18 (30)	7.7 ± 0.1	12.6 ± 0.2	12.6
	19 (≡100)	5.6 ± 0.1	10.5 ± 0.2	
	20 (0.6)	5.9 ± 0.3	10.8 ± 0.4	
	32 (0.4)	7.0 ± 0.2	11.9 ± 0.3	
	36 (20)	6.6 ± 0.2	11.5 ± 0.3	
	37 (80)	5.5 ± 0.2	10.4 ± 0.3	
	50 (0.3)	7.1 ± 0.3	12.0 ± 0.4	

Table III.

Substance	Ion (m/e)	ΔU (eV)	AP (eV)	IP (eV)
Methanol	30 (3)	6.4 ± 0.2	11.3 ± 0.3	
		3.6 ± 0.3	8.5 ± 0.4	
	31 (6)	3.0 ± 0.2	7.9 ± 0.3	
	32 (26)	6.0 ± 0.1	10.9 ± 0.2	10.9
	33 (≡100)	4.0 ± 0.2	8.9 ± 0.3	
	63 (0.9)	3.9 ± 0.3	8.8 ± 0.4	
	65 (17)	3.3 ± 0.2	8.2 ± 0.3	

contain a proportion due to the ^{13}C isotope content of $CH_2O^{\cdot+}$, CH_2OH^+, and $CH_3OH^{\cdot+}$, which is in each case 0.5% of the intensity of the previous mass number, or less. These intensities are too small to have any influence on the determination of the cut-off point.

Discussion

Energy Distribution and APs of Molecular Ions

The retardation curves of the molecular ions have the same shape as those of the noble gas ions. This implies that the energy distributions of these ions reveal no essential differences. The sharpness of the ion signal cut-off observed despite the large relative retardation employed indicates that the ion energy distribution possesses a sharp intensity maximum at this point.

The APs of the paraffin ions lie above the adiabatic IP of the paraffins which is a result of the energy transfer during FI. For noble gases the energy distribution is approximately given by the tunneling probability alone. However, for the energy distribution of molecules we have:

$$P(E) \sim D(E)\, f(\varepsilon)\, \varrho(\varepsilon) \qquad (3)$$

with $E = \mathrm{IP} + \varepsilon$, where $f(\varepsilon)$ is a function which describes the dependence of the Franck-Condon factor on the internal exitation energy ε of the ion and $\varrho(\varepsilon)$ is the density of states of the ion. In particular for paraffins $f(\varepsilon)$ and $\varrho(\varepsilon)$ nearly vanish for $\varepsilon = 0$ [12]. Both functions increase with a very high power of ε. Thus the maximum of the energy distribution in (3) is no longer at the adiabatic ionization potential, but at a value $E = \mathrm{IP} + \varepsilon$, where $\varepsilon > 0$. Under these conditions AP measurements do not give the adiabatic IP, but a value which is shifted to higher energies. In the case of n-heptane the AP measurements indicate a sharp maximum in the energy deposition function at a few tenths of an eV. (A detailed discussion of equation (3) and of the energy transfer during FI will appear elsewhere.)

The Fragment Ions of n-Heptane

A flattened fragment ion retardation curve is to be expected when the fragment ions are produced by a fast monomolecular decomposition, i.e. by field dissociation of the molecular ion. A flattened curve of this type is only clearly observable in the case of the $C_2H_5^+$ ion of mass 29 (Figure 5). $C_2H_5^+$ ions

are produced by field dissociation of heptane molecular ions [13]. The AP of monomolecular decomposition products must lie above the IP of the molecule. However, the APs of the fragment ions of heptane all lie below the IP of the molecule. It follows that the $C_3H_7^+$, $C_4H_9^+$, $C_5H_{11}^+$ and a small proportion of the $C_2H_5^+$ ions are produced largely by reactions other than monomolecular decompositions.

$C_5H_{11}^+$ and also $C_4H_9^+$ ions (with much lower intensity) may originate from the FI of neutral radicalic field dissociation products. If we assume a decomposition of the radicals, then $C_2H_5^+$ and $C_3H_7^+$ ions may also be produced. This enables the low APs of the alkyl ions to be partially explained, since the IPs of the radicals are between 8.0 and 8.4 eV. However, the intensity distribution of the alkyl ions is difficult to explain using this assumption. Thus the origin of the alkyl ions in the n-heptane spectrum remains partially unclear.

Protonation Reactions

The AP of H_3O^+ for the FI of water at W was determined by Anway to be 8.8 eV. This results from the participation of the surface in the proton transfer reaction, i. e. simultaneously with the proton transfer the remaining OH· radical is bound to the emitter surface [14]:

$$2\,H_2O \xrightarrow{-e} *OH + H_3O^+ . \qquad (4)$$

A similar reaction mechanism must also operate during the production of the H_3O^+ ion at Pt, since the AP of 10.5 eV is below that of the reaction:

$$2\,H_2O \xrightarrow{-e} OH^{\cdot} + H_3O^+ \qquad (5)$$

in physically adsorbed layers. The AP of the H_3O^+ ions in (5) is calculated from the ionization potential of H_2O and the difference of the proton affinities (PA) of H_2O (7.1 eV) [15] and OH· (6.2 eV) [16], and is 11.7 eV if the effect of the adsorption energies is ignored. A value of 1.1 eV for the binding energy of the OH· radical to the Pt surface is obtained from (4). This binding energy is not necessarily that of a Pt-OH bond, but probably the binding energy of the OH· radical to a radicalic center of a contaminated Pt surface.

The situation of the $H_2O \cdot H_3O^+$ ion is the same as that of the H_3O^+ ion, since the proton affinity of $(H_2O)_2$ is probably only slightly different from that of the H_2O molecule itself.

The AP of the $(2\,H_2O)^+$ ion corresponds approximately to that of the reaction (5), i. e. the dimeric water ion is a product of the proton transfer reaction:

$$2\,H_2O \xrightarrow{-e} (OH^{\cdot}\,H_3O)^+ . \qquad (6)$$

This structure of $(2\,M)^+$ dimers has already been suggested [17].

The AP of the $(M+H)^+$ ion of methanol is about 2 eV below that of the methanol molecular ion. For the reaction:

$$2\,CH_3OH \xrightarrow{-e} CH_3O^{\cdot} + CH_3OH_2^+ + \Delta E . \qquad (7)$$

ΔE is determined to be 10.2 eV with $D\,(CH_3O-H) = 4.4$ eV [18] and PA $(CH_3OH) = 7.8$ eV [19]. It follows that the protonation of CH_3OH must also occur by an analogous reaction mechanism to that of (4), in which the emitter surface is chemically active. The flattened shape of the retardation curve of m/e 33 is produced by the superimposition of several processes, i. e. the additional contributions of the reaction (7) and the field dissociation of $(2\,M+H)^+$ ions.

The same conditions which apply to the $(M+H)^+$ ion of methanol should also apply to the $(2\,M+H)^+$ ions. However, the large difference in the APs of m/e 65 and m/e 33 remains puzzling.

Hydrogen Elimination Reactions

The CH_3^+ ion in the methane spectrum does not result from field dissociation of CH_4^+, but is produced by the surface reaction [17]:

$$CH_4 \xrightarrow{-e} *H + CH_3^+ . \qquad (8)$$

The AP (CH_3^+) of 10.8 eV leads to an estimated binding energy $D\,(*H)$ of about 3.6 eV with $D\,(CH_3-H) = 4.5$ eV and IP $(CH_3^{\cdot}) = 9.8$ eV [9]. This value lies above the Pt-H binding energy, and indicates a reaction with radicals in the adsorption layers on the emitter. These radicals may be formed by an interaction of water molecules of the residual gas with the Pt surface.

The CH_2OH^+ and CH_2O^+ ions of the methanol spectrum also result from hydrogen elimination reactions. The structure of the former ion was determined by Goldenfeld et al. [20] by deuterium labelling. If the lower AP of CH_2OH^+ is attributed

to the reaction:

$$CH_3OH \xrightarrow{-e} *H + CH_2OH^+, \qquad (9)$$

the AP (CH_2OH^+) of 7.9 eV leads to a binding energy $D(*H)$ of about 4.3 eV which, however, is unreasonably high. The following reaction is more likely:

$$CH_3O^\cdot + CH_3OH \xrightarrow{-e} CH_3OH + CH_2OH^+, \qquad (10)$$

in which the $CH_3O^\cdot$ radical is produced by the proton transfer reaction (7). Using this reaction with

$$IP(CH_2OH^\cdot) \cong 8.2 \text{ eV}\ [16] \text{ and}$$
$$D(CH_3O-H) - D(H-CH_2OH) \cong 0.4 \text{ eV}\ [18],$$

an AP for CH_2OH^+ of 7.8 eV is calculated. This agrees well with the measured AP value within the accuracy of the experiment. The second and higher AP of m/e 31 should apply to the field dissociation of the molecular ion:

$$CH_3OH^+ \xrightarrow{\text{field}} CH_2OH^+ + H^\cdot. \qquad (11)$$

The mass signal at m/e 31 is correspondingly broadened [21]. In addition the AP for the field free decomposition reaction analogous to (11) is about 12.2 eV.

The steps in the retardation curve of m/e 30 indicate a second ion production process once again. If we ascribe the AP of 8.5 eV to the reaction:

$$CH_3O^\cdot \xrightarrow{-e} *H + CH_2O^+ \qquad (12)$$

where $IP(CH_2O) = 11.9$ [9] and $D(^\cdot OCH_2-H) \cong 1.1$ eV [16] the $*H$ bond strength is determined to be about 3.5 eV. This value agrees with that found for reaction (8) indicating once more the effect of water layers.

The second AP of CH_2O^+ (≈ 11.1 eV) is in the region of the IP of CH_2O. CH_2O molecules can be produced by hydrogen elimination from $CH_3O^\cdot$ or by a catalytic oxidation of methanol molecules at the Pt emitter surface. In this case the field ionization would be a secondary process.

The $(2M-H)^+$ Ion of Methanol

There are several possible structures for the $(2M-H)^+$ methanol ion: $CH_3-O^+H-CH_2OH$, $CH_3OCH_2O^+H_2$ and $CH_3-HO^+-OCH_3$, of which the last is the most likely, since $(2M-H)^+$ ions may be produced by a simple addition reaction:

$$CH_3OH + CH_3O^\cdot \xrightarrow{-e} CH_3OHOCH_3^+. \qquad (13)$$

The $O-O^+$ binding energy which corresponds to $IP(CH_3OH) - AP(2M-H)^+$, is calculated to be 2 eV from the AP of 8.9 eV. This value is of the same order of magnitude as that of O – O bonds.

Conclusion

The examples discussed above show clearly that the AP can shed light on the mechanisms of field ion production. The low APs of the protonated water and methanol molecules and of the CH_3^+ ion of methane indicate a participation of the emitter surface in the ion production mechanisms. However, the platinum surface itself does not appear to be directly involved in the ion production; the adsorbate covered surface is active. Several processes are involved in the generation of $(M-H)^+$ and $(M-2H^\cdot)^+$ ions from methanol. The low values of the measured APs of the fragment ions of n-heptane demonstrate that alkyl ions are not only produced by monomolecular decomposition of the molecular ion. The generation mechanism of these ions could not be elucidated. In the case of paraffins the APs of the molecular ions allow conclusions to be drawn about the energy deposition function at small energies. The measurements confirm the former results [14, 17], that field reactions do not require activation energy, i. e. they are nearly adiabatic. No evidence of the dependence of the AP on the adsorption layers present on the surface was found. Whether this is also true for larger organic molecules must still be investigated.

Acknowledgement

The authors are grateful to the Deutsche Forschungsgemeinschaft for financial support.

[1] A. J. Jason, Phys. Rev. **156**, 266 [1967].
[2] E. W. Müller and S. V. Krishnaswamy, Surface Sci. **36**, 29 [1973].
[3] A. R. Anway, J. Chem. Phys. **50**, 2012 [1969].
[4] A. J. Jason, B. Halpern, M. G. Inghram, and R. Gomer, J. Chem. Phys. **52**, 2227 [1970].
[5] F. W. Röllgen and H. D. Beckey, 18th Field Emission Symposium, Eindhoven 1971.
[6] H. J. Heinen, Diplomarbeit, Bonn 1972.
[7] T. T. Tsong and E. W. Müller, J. Chem. Phys. **41**, 3279 [1964].
[8] J. Block, H. Thimm, and M. S. Zei, Ind. Chim. Belg. **38**, 392 [1973].
[9] J. L. Franklin, J. G. Dillard, H. M. Rosenstock, J. T. Herron, K. Draxl, and F. H. Field, Ionization Potentials, Appearance Potentials and Heats of Formation of Gaseous Positive Ions, NSRDS-NBS 26, Washington 1969.

[10] B. Brehm, Z. Naturforsch. **21 a**, 196 [1966].
[11] W. A. Schmidt, Z. Naturforsch. **19 a**, 318 [1964].
[12] B. Steiner, C. F. Giese, and M. G. Inghram, J. Chem. Phys. **34**, 189 [1961].
[13] H. D. Beckey, Field Ionization Mass Spectrometry, Pergamon Press, Oxford, New York 1971.
[14] F. W. Röllgen and H. D. Beckey, Surface Sci. **27**, 312 [1971].
[15] J. Long and B. Munson, J. Chem. Phys. **53**, 1356 [1970].
[16] V. I. Vedeneyev, L. V. Gurvich, V. N. Kondrat'yev, V. A. Medvedev, and Ye. L. Frankevich, Bond Energies, Ionization Potentials and Electron Affinities, Edward Arnold Ltd., London 1966.
[17] F. W. Röllgen and H. D. Beckey, Z. Naturforsch. **29 a**, 230 [1974].
[18] Handbook of Chemistry and Physics, The Chemical Rubber Co., Cleveland 1969.
[19] S. L. Chang and J. L. Franklin, J. Am. Chem. Soc. **94**, 6347 [1972].
[20] I. V. Goldenfeld and I. Z. Korostyshevsky, Theoret. Eksp. Khim. **4**, 218 [1968].
[21] H. D. Beckey and P. Schulze, Z. Naturforsch. **21 a**, 214 [1966].